

Use of the Routing Procedure to Study Dye and Gas Transport in the West Fork Trinity River, Texas

United States
Geological
Survey
Water-Supply
Paper 2252



Use of the Routing Procedure to Study Dye and Gas Transport in the West Fork Trinity River, Texas

By H. E. JOBSON and R. E. RATHBUN

U.S. GEOLOGICAL SURVEY WATER-SUPPLY PAPER 2252

DEPARTMENT OF THE INTERIOR
WILLIAM P. CLARK, Secretary

U.S. GEOLOGICAL SURVEY
Dallas L. Peck, Director



UNITED STATES GOVERNMENT PRINTING OFFICE: 1984

For sale by the Distribution Branch, U.S. Geological Survey,
604 South Pickett Street, Alexandria, VA 22304

Library of Congress Cataloging in Publication Data

Jobson, Harvey E.
Use of the routing procedure to study dye and gas transport
in the West Fork Trinity River, Texas

(U.S. Geological Survey water-supply paper ; 2252)

Bibliography: p.

Supt. of Docs. no. : I 19.13:2252

1. Stream measurements--Texas--Trinity River, West
Fork. 2. Diffusion in hydrology. 3. Gases--Absorption
and adsorption. I. Rathbun, R.E. II. Title.
III. Title: Routing procedure to study dye and gas
transport. IV. Series

GB1225.T4J62 1984 551.48'3'097628 83--600333

CONTENTS

List of symbols	IV
Abstract	1
Introduction	1
Acknowledgments	2
The river reach	2
Model development	3
Results	7
Dispersion	7
Desorption	16
Evaluation of the model	18
Summary and conclusions	19
References	19
Metric conversion factors	21

FIGURES

1. West Fork Trinity River and data-collection points 3
2. Bed profile for West Fork Trinity River and water-surface profiles for September and November flows 6
3. Comparison of observed peak dye and gas concentrations and computed concentrations, West Fork Trinity River downstream from Route 820 8
4. Time variation of observed and computed dye concentrations in the West Fork Trinity River downstream from Route 820 10
5. Comparison of observed peak dye and gas concentrations and computed concentrations, West Fork Trinity River downstream from Fossil Creek 11
6. Time variation of observed and computed dye concentrations in the West Fork Trinity River downstream from Fossil Creek 12
7. Comparison of observed peak dye and gas concentrations and computed concentrations, West Fork Trinity River downstream from Beach Street 13
8. Time variation of observed and computed dye concentrations in the West Fork Trinity River downstream from Beach Street 14
9. Variation of root-mean-square error in predicted peak dye concentrations as a function of the dispersion coefficient 15
10. Variation of the dispersion coefficient with mean stream velocity in the West Fork Trinity River 16

TABLES

1. Reconnaissance data for West Fork Trinity River, September 3-4, 1980 4
2. Summary of data obtained on the West Fork Trinity River, November 10-13, 1980 9
3. Results of model calibration on West Fork Trinity River 17

LIST OF SYMBOLS

A	Local cross sectional area of the river
c	Concentration
c_i	Concentration of a particular constituent i
$c_{ri,k}$	Reference or equilibrium concentration of constituent k at which the production of constituent i is zero
$d\xi$	Distance between parcels
D_x	Longitudinal dispersion coefficient
D_f	Dispersion factor
m_r	Liquid film coefficient for ethylene
Q	Discharge
t	Time
u	Velocity
V	Volume of the parcel
W	Local top width of water surface
x, x_o	Locations of the parcel at time t and t_o , respectively
$xk_{i,k}$	Kinetic exchange coefficient for the production of constituent i due to the presence of constituent k
Δc_d	Change in concentration due to dispersion between the parcel and each of its neighbors
Δc_x	Concentration difference between adjacent parcels at the old time step
Δt	Time step size
ξ	Distance from parcel
ϕ	Rate of increase of concentration due to point input sources

Use of the Routing Procedure to Study Dye and Gas Transport in the West Fork Trinity River, Texas

By H. E. JOBSON and R. E. RATHBUN

Abstract

Rhodamine-WT dye, ethylene, and propane were injected at three sites along a 21.6-kilometer reach of the West Fork Trinity River below Fort Worth, Texas. Complete dye concentration versus time curves and peak gas concentrations were measured at three cross sections below each injection. The peak dye concentrations were located and samples were collected at about three-hour intervals for as many as six additional cross sections. These data were analyzed to determine the longitudinal dispersion coefficients as well as the gas desorption coefficients using both standard techniques and a numerical routing procedure.

The routing procedure, using a Lagrangian transport model to minimize numerical dispersion, provided better estimates of the dispersion coefficient than did the method of moments. At a steady flow of about $0.76 \text{ m}^3/\text{s}$, the dispersion coefficient varied from about $0.7 \text{ m}^2/\text{s}$ in a reach contained within a single deep pool to about $2.0 \text{ m}^2/\text{s}$ in a reach containing riffles and small pools.

The bulk desorption coefficients computed using the routing procedure and the standard peak method were essentially the same. The liquid film coefficient could also be obtained using the routing procedure. Both the bulk desorption coefficient and the liquid film coefficient were much smaller in the pooled reach than in the reaches containing riffles.

INTRODUCTION

The U.S. Geological Survey in cooperation with the U.S. Army Corps of Engineers and the Texas Department of Water Resources conducted an intensive water-quality data collection effort on the West Fork Trinity River on November 10-14, 1980. As part of this effort, reaeration coefficients were estimated using the modified tracer technique (Rathbun and others, 1975) on the 21.6-kilometer

reach beginning at Fort Worth, Tex. The tracer technique involves injecting a fluorescent dye as well as ethylene and propane into the river for a short time and then observing the variation of peak concentrations with distance downstream.

This report presents the dispersion and desorption coefficients inferred from these data and illustrates the use of a Lagrangian transport model to determine dispersion and desorption coefficients by routing techniques. Results are compared with those obtained by standard procedures. The routing technique is shown to be as accurate as standard procedures and to offer much more flexibility for data interpretation.

The usual procedure for computing the dispersion coefficient from time-of-travel data is to apply the method-of-moments (Fischer, 1968). When even a small amount of dye is temporarily trapped in slow-moving water, such as near river banks, and then is released to the main flow, the rate at which the concentration approaches zero with time is reduced (a tail is added to the concentration versus time curve). This tail greatly increases the dispersion coefficient computed by the method-of-moments. According to Yotsukura, Fischer, and Sayre (1970), the large effect of these tails is the major difficulty in computing the dispersion coefficient by the method-of-moments.

In the routing procedure, the convective-dispersion equation is solved, and the dispersion coefficient is inferred as that value which allows the equation to best represent the observed dye concentrations. According to Yotsukura, Fischer, and Sayre (1970), the routing procedure is least sensitive to both human judgement and data scatter and produces a coefficient that more nearly matches the data than any of the several methods available. Numerical models based on the usual Eulerian reference frame generally contain so much numerical dispersion that their use with a routing procedure is not recommended.

The desorption coefficients of dissolved gases are inferred from the rate of decrease in the peak gas concentrations in relation to the rate of decrease in the peak dye concentration with distance downstream. The standard analysis procedure (the peak method) involves plotting the logarithm of the ratio of the peak gas to dye concentrations against time of travel and fitting a straight line to the plotted points. The slope of the line is the desorption coefficient.

The routing procedure involves modeling the gas concentrations with a convective dispersion equation that allows for gas transfer at the air-water interface. The dispersion coefficient in the model is first determined such that the dye concentrations are accurately modeled. The desorption coefficient is then determined such that the model best represents the observed gas concentrations.

The standard procedures, or the routing procedure using analytic solutions, are very restrictive in that all coefficients and conditions must be assumed to be uniform and local influences such as tributary inflow must be either ignored or accounted for separately. The routing procedure using a general numerical solution to the transport equation, however, can be very flexible and allow coefficients and conditions to vary with time and distance. Desorption or dispersion coefficients can be represented as functions of hydraulic or meteorologic variables, and the constants in the assumed functional relations can be determined rather than the coefficients themselves.

The paper begins with an explanation of the river reach. This is followed by an explanation of the model used in data analysis and a discussion of model's accuracy. The dispersion coefficient for each injection is then determined using both the method-of-moments and the routing procedures. Finally, the desorption coefficients are determined, and the results discussed.

ACKNOWLEDGMENTS

The overall study was the joint effort of personnel from the U.S. Army Corps of Engineers, the Texas Department of Water Resources, and the U.S. Geological Survey. M. E. Jennings was project chief, and S. C. McCutcheon supervised and coordinated the field study. Personnel assisting with the field aspects of the dye and gas transport study were David Buzan and Lynn Coles of the Texas Department of Water Resources and Roy Hastings and Craig Henley of the U.S. Geological Survey. The Fort Worth and Austin offices of the U.S. Geological Survey provided logistical support. John Vaupotic of the Atlanta Central Laboratory of the U.S. Geological Survey did the gas analyses, and Gala Goldsmith of the U.S. Geological Survey assisted with the dye analyses. Craig Henley, Leslie Rush, Diana Horton, and Joni Devitt of the U.S. Geological Survey assisted with the data analysis.

THE RIVER REACH

A preliminary reconnaissance trip down the river was conducted on September 3-4, 1980. A crew of three traversed the reach in a small boat during conditions of steady but extremely low flow of about 0.06-0.14 m³/s. Notes on the general character of the river were taken, and 23 cross sections of pooled reaches (including 18 surveyed sections available from the Corps of Engineers) were located on topographic maps. A range finder was used to determine the surface width, and the mean water depth was estimated as the average of five equally spaced soundings. The locations of riffled sections were also noted. The water-surface altitude was determined at Beach Street, First Street, and the Hadley-Edderville Road (see fig. 1).

The river consists of a series of pools separated by riffled sections. In general, riffled sections occur downstream of side washes which appear to have deposited large quantities of coarse material in the river. The deposits block the river, causing the deep upstream pools. Riffled sections are frequently quite long and consist of a series of small riffles separated by pools of varying sizes. The distance between the banks, as well as bank height above the water surface, remains more or less uniform throughout. The data recorded during the reconnaissance are presented in table 1. The reach was terminated just upstream of Randol Mill Road because of an abandoned low-water crossing there which served as a major control structure.

Figure 1 is a location sketch of the river showing river miles, locations where dye and gas samples were taken, and major landmarks. Three injections were made to determine the gas desorption coefficients. On November 10, 11, and 12, 1980, rhodamine-WT dye, ethylene, and propane were injected into the river for about 1 hour near Route 820, Fossil Creek, and Beach Street, respectively. Complete dye concentration time curves were obtained at sample points A, B, and C downstream of each injection (fig. 1). Gas samples were obtained for later analysis as the peak of the dye cloud passed each sample point. After the dye had passed sample point C, the peak dye concentration was located in the river at about 3-hour intervals by slowly drifting through the dye cloud and making frequent concentration measurements. When the peak was found, samples were collected for later analysis and the location of the sample point was marked on the river bank so the river mile could be determined later. The locations of these sampling points are indicated by the letters D, E, F, and so forth, in figure 1.

Considering the data available and the amount of detail that was practical to include in a mathematical model, it was decided to represent the reach by 10 riffled sections separated by pools. For modeling purposes, 50 grid points were used. A grid point was placed at each end of the riffled sections and at each end of the pools, allowing a transition between. Some pools contained addi-

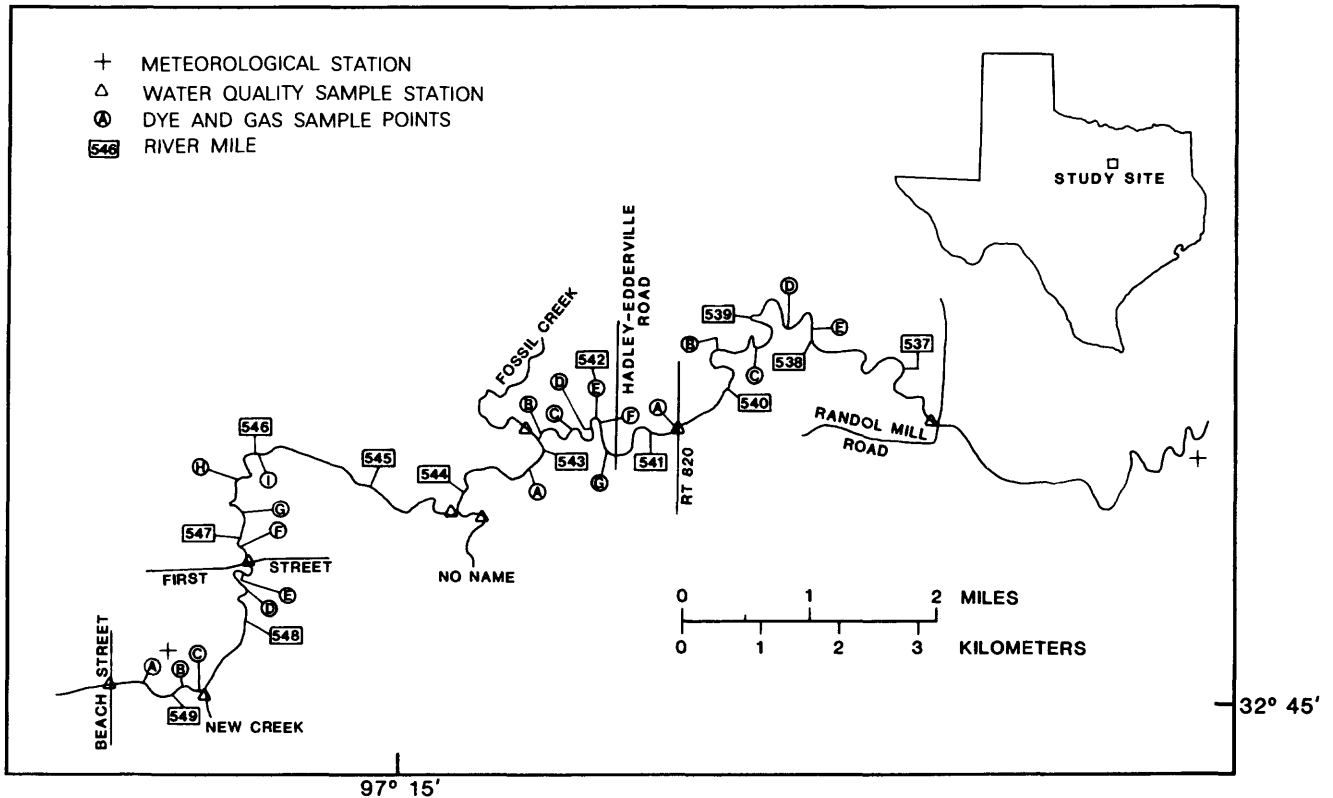


Figure 1. West Fork Trinity River and data-collection points.

tional grid points if data were available. The bed profile of the river is shown in figure 2. The grid points show up as sharp breaks in slope. The location of each injection point is indicated by a small arrow, and the location of each sample point is indicated by a letter.

Since only steady flow is considered here, an unsteady flow model was not necessary. A Mannings roughness coefficient of 0.06 was assumed for the riffled sections. The cross sections provided by the Corps of Engineers contained roughness values for the pools that ranged from 0.045 to 0.050. The cross-sectional areas in the riffles were set to values that reproduced the water-surface elevations observed during the run. The areas of the pools were set to values necessary to reproduce the observed travel times or were inferred from the observations in table 1.

A water-surface profile for a flow representative of November 10-14, 1980, was computed from the known areas and roughness values and was plotted, as shown in figure 2. The bed profile shown in figure 2 was determined such that the cross-sectional shape yielded the known area at the computed water-surface altitude. The bed altitude is represented as the deepest point in the cross section. A water-surface profile representative of the flow

on September 3-4, 1980, was then computed, and the results were compared with the observed water-surface altitudes (fig. 2).

MODEL DEVELOPMENT

The Lagrangian transport model documented by Jobson (1981) was used to simulate the movement of dye and dissolved gases in the study reach. In the Lagrangian reference frame, one conceptually follows an individual fluid parcel while keeping track of all factors that act to change its concentration. The equation of continuity is

$$\frac{\partial c}{\partial t} = \frac{\partial}{\partial \xi} \left(D_x \frac{\partial c}{\partial \xi} \right) + xk(c - c_r) + \phi \quad (1)$$

where c =concentration, t =time, ξ =distance from the parcel, D_x =longitudinal dispersion coefficient, xk =kinematic exchange coefficient describing the production (or loss) of concentration, c_r =reference or equilibrium concentration, and ϕ =rate of increase of concentration due to point input

Table 1. Reconnaissance data for West Fork Trinity River, September 3-4, 1980

Location, in river miles	Top width, in meters	Average depth, in meters	Discharge, in cubic meters per second	Water- surface altitude, in meters	Notes
549.60*	12.5	0.27	0.06	147.04	Beach Street.
549.40*	17.4	.88			Beginning pooled reach.
549.11*	21.6	1.19			
549.00					Rock outcrop.
548.89*	21.6	1.55			
548.73					Begin riffles.
548.52*	12.2	0.73			Small pool.
548.15					Begin pooled reach.
547.21*	15.2	1.10		144.05	First Street.
546.70*	12.2	1.37			
546.44					Begin riffles.
546.35			0.08		End riffles.
545.97*	9.1	0.34			
545.8	12.2	1.07			
545.45*	18.0	1.34			
544.30*	16.5	2.04			
544.21					Begin riffles.
543.81					End riffles.
543.74	12.2	0.85			
543.41					Begin riffles.
543.08*	9.1	0.30			Small pool.
542.97					End riffles.
542.87	23.2	1.31			Begin pools just upstream of Fossil Creek.

*U.S. Army Corps of Engineers section.

sources such as tributaries. The Lagrangian distance coordinate ξ is given by

$$\xi = x - x_0 - \int_{t_0}^t u \, dt \quad (2)$$

where $\xi=0$ for the particular parcel at any time, x and x_0 are the locations of the parcel at time t and t_0 , respectively, and u =velocity. The finite difference solution is constructed by starting with a number of parcels distributed along the river reach and adding a new parcel to the upstream boundary at each time step. The three terms on the right of equation 1 quantify the rate of change of concentration in the parcel due to dispersion, decay, and point sources, respectively. These terms are evaluated individually during each time step.

The dispersion term is evaluated by use of an explicit finite difference approximation in which the distance between parcels ($d\xi$) is set equal to the velocity times the time step size Δt . During the time step, the change in concentration due to dispersion between the parcel and each of its neighbors, Δc_d , is computed as

$$\Delta c_d = \frac{D_x}{u^2 \Delta t} \Delta c_x \quad (3)$$

in which D_x = dispersion coefficient evaluated at the boundary between the parcels and Δc_x = concentration difference between adjacent parcels at the old time step. For use in real rivers, the right side of equation 3 is multiplied by $Q\Delta t/V$ in which Q = discharge and V = volume of the parcel. This

Table 1. Reconnaissance data for West Fork Trinity River, September 3–4, 1980—Continued

Location, in river miles	Top width, in meters	Average depth, in meters	Discharge, in cubic meters per second	Water- surface altitude, in meters	Notes
541.58*	20.7	0.94	0.14	141.66	Hadley-Edderville Road.
541.53					Begin riffles.
541.43					End riffles.
541.14*	20.1	0.70			
540.80*	22.9	0.37			Route 820.
540.73					Begin riffles.
540.58					End riffles.
540.41*	17.1	1.16			
540.28					Begin riffles.
540.17					End riffles.
539.69*	12.2	0.91			
539.20					Begin riffles, clay bed.
538.93					End riffles, clay bed.
538.48					Begin riffles.
538.43					End riffles.
538.41*	16.2	0.67			
538.30					Begin riffles.
537.75					End riffles.
537.69*	9.1	0.37			
537.62					Begin riffles.
537.37					End riffles.
537.05	17.7	1.01			
536.16	16.5	1.10			Upstream of Randol Mill Road.

* U.S. Army Corps of Engineers section.

ratio, which is unity for steady flow, forces the finite difference approximation to conserve mass even for highly unsteady, non-uniform flow where the parcel volume changes owing to diversion or tributary inflow.

The approximation in equation 3 is not exact but contains some numerical dispersion. The accuracy of the solution is a function of the dimensionless dispersion factor, D_f , where

$$D_f = \frac{D_x}{u^2 \Delta t} = \left(\frac{(D_x \Delta t)^{1/2}}{u \Delta t} \right)^2 \quad (4)$$

The dispersion factor, and therefore the accuracy of the solution, can be controlled by the modeler through the selection

of the time step Δt . The distance between parcels is $u \Delta t$ and $(D_x \Delta t)^{1/2}$ is the distance scale used to nondimensionalize analytical solutions for diffusion in solids (Carslaw and Jaeger, 1959). The dispersion factor has physical significance because it is the square of the ratio of the length scale of the diffusive process to the distance between parcels. The optimum accuracy can be shown empirically to occur at $D_f = 0.2$.

The accuracy of the Lagrangian model in simulating analytic solutions to the convective dispersion equation has been demonstrated (Jobson, 1980), but the real test of concern here is the ability of the model to infer the dispersion coefficient from observed or predicted concentration data. To check the model's accuracy in this regard, concentrations were predicted for two points downstream of an instantaneous plane source in a uniform channel with

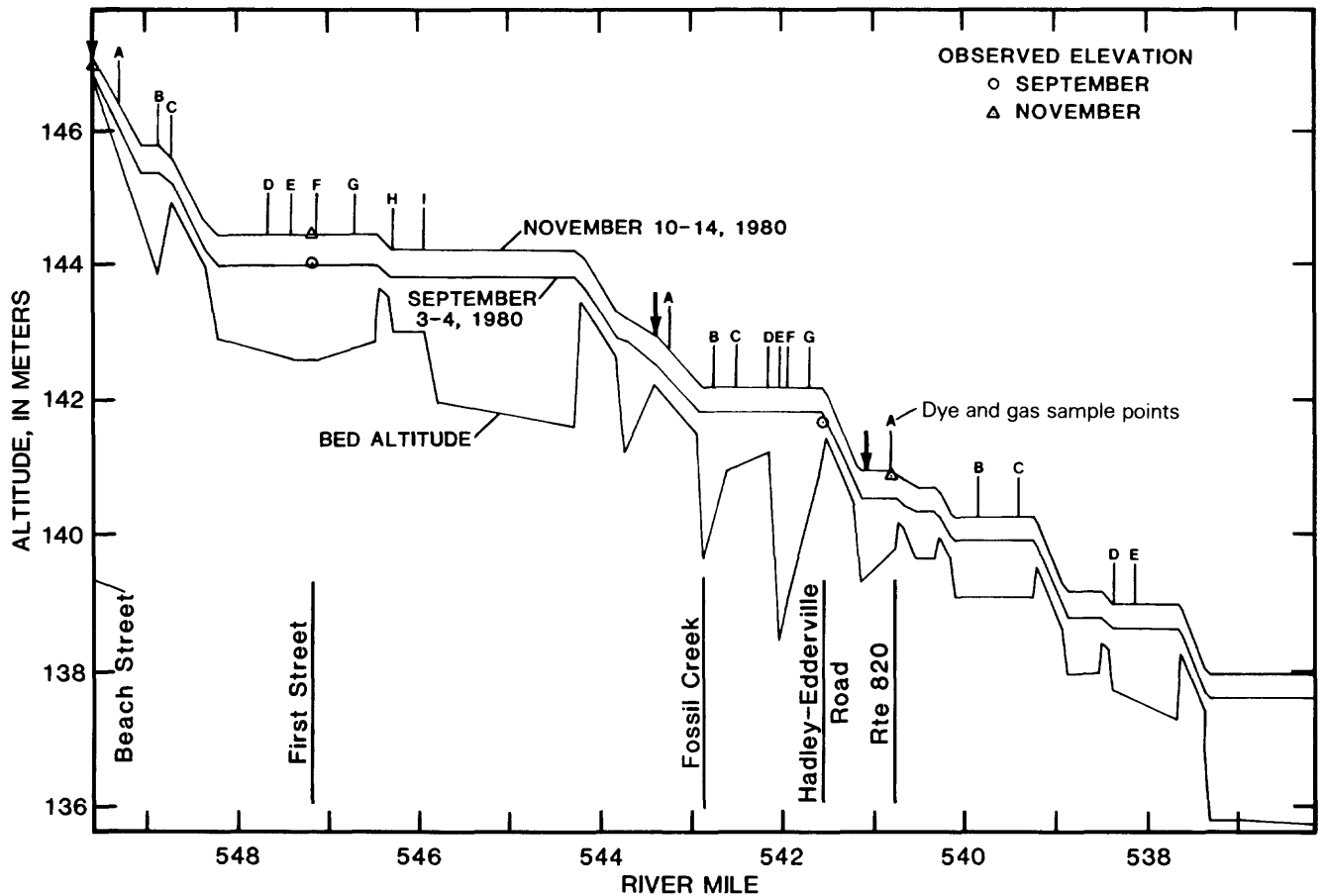


Figure 2. Bed profile for West Fork Trinity River and water-surface profiles for September and November flows.

steady flow using the well-known convolution solution. These “exact” concentrations were then used as the upstream and downstream boundary conditions in the model, and the dispersion coefficient was inferred as the value that minimized the root-mean-square (RMS) error between the predicted and “exact” concentration at the downstream boundary. Various dispersion coefficients, velocities, and distances downstream of the source were used in the test. Likewise, the time step size in the model was varied so that the dispersion factor in equation 4 varied from 0.06 to 0.40. In all cases, the model extracted the dispersion coefficient to within ± 3.8 percent, as long as the sections were separated by a travel time equivalent to at least 15 time steps. For the extremely non-uniform conditions in the Trinity River, it was shown that increasing the dispersion factor from about 0.2 to 0.4 by reducing the time step size by a factor of two affected the computed optimum dispersion coefficient by less than 15 percent.

Complete concentration-time curves are difficult to obtain in the field. Likewise, processes other than diffusion have the largest relative effect on the lower part of the dye curves measured in the field. Since the peak concentration contains more information than any other point on the dye curve, it was decided to see how accurately the dispersion coefficient could be extracted from data by simply matching the computed and observed peaks at the downstream site. For the cases tested using the analytically predicted curves, the error in the dispersion coefficient, obtained by matching the downstream peak concentrations, varied from -3.0 percent to $+5.6$ percent. Field data obtained on the Missouri River by Yotsukura and others (1970) were also analyzed to determine if the dispersion coefficient obtained by fitting the complete curve differed significantly from the value obtained by fitting only the peak concentration. The Missouri River data contained four complete concentration versus time curves

over the 162-kilometer reach. The dispersion coefficient obtained by fitting only the peak concentrations differed by less than 10 percent from the value obtained when the complete concentration curves were used. Considering the large variability in dispersion coefficients usually observed from run to run, it was concluded that the dispersion coefficient could be obtained with sufficient accuracy using the routing procedure and only the peak dye concentrations obtained downstream of a single complete concentration-time curve.

The model also allows simulation of as many as 10 interacting constituents at one time. For purposes of the model, equation 1 is written as

$$\frac{\partial c_i}{\partial t} = \frac{\partial}{\partial \xi} \left(D_x \frac{\partial c_i}{\partial \xi} \right) + \phi_i + \sum_{k=1}^{10} xk_{i,k} (c_k - c_{r1,k}) \quad (5)$$

in which c_i =concentration of a particular constituent, $xk_{i,k}$ =kinetic exchange coefficient for the production of constituent i due to the presence of constituent k , and $c_{r1,k}$ =reference concentration of constituent k at which the production is zero.

For the Trinity River study, only three components were simulated: $k=1$ for dye, $k=2$ for ethylene, and $k=3$ for propane. Two models of the surface exchange were tested, however. The first model, the bulk-transfer model, is based on the assumption that desorption is a first order process. Writing equation 5 for ethylene, for example, gives

$$\frac{\partial c_2}{\partial t} = \frac{\partial}{\partial \xi} \left(D_x \frac{\partial c_2}{\partial \xi} \right) + \phi_2 + xk_{2,2} (c_2 - c_{r2,2}) \quad (6)$$

in which c_2 =concentration of ethylene in the water at time t , $c_{r2,2}$ =concentration of ethylene in the water when the water is at equilibrium with the air above the water, and $xk_{2,2}$ =negative of the desorption coefficient with units of inverse time. All values of xk and c_r are zero if $i \neq k$. For solutes such as ethylene or propane that are not normally present in the air, the value of $c_{r1,i}$ can also be assumed to be zero.

The surface exchange was also modeled as a mass-transfer process in which the liquid film coefficient, m_T , is the parameter that quantifies the gas transfer. In applying the mass-transfer model, the value of $xk_{2,2}$ in equation 6 is given by

$$xk_{2,2} = \frac{m_T W}{A} \quad (7)$$

in which m_T =liquid film coefficient for ethylene in units of length/time, W =local top width of water surface, and A =local cross-sectional area of the river. The values of W and A were assumed constant between grid points in the model but changed as the parcel passed each grid point.

RESULTS

Dispersion and desorption coefficients were determined by injecting dye as well as ethylene and propane into the river and then monitoring the rate of decrease of concentrations as they moved downstream. At the first three points downstream of each injection (points A, B, and C in figs. 1 and 2), a complete dye concentration versus time curve was obtained, and gas concentrations were determined at the time of the peak dye concentration. At all other stations, only single samples representing the peak dye and gas concentrations were taken. The flow was steady at 0.76 m³/s during all runs.

Dispersion

The first step in the analysis was to determine the dispersion coefficient by the routing procedure. Using the observed dye concentration at point A as the upstream boundary condition, the dispersion coefficient in equation 3 was found such that the RMS error between the computed and observed peak dye concentrations for all downstream points was a minimum. This procedure yields the dispersion coefficient that best fits all peak data in the RMS sense. A comparison of the computed and observed peak dye concentrations for the Route 820 injection is shown in figure 3. The figure also contains computed concentration versus distance profiles for specific times that are slightly different from the observed peak times. The modeled and observed results do not occur at exactly the same time because the model time step was 30 minutes and observed peak concentrations did not necessarily occur at the times of the model output. The model does an excellent job of simulating the reduction in peak dye concentration with distance downstream of the Route 820 injection. The optimum results were obtained with a dispersion factor of 0.27 ± 0.01 . Using the mean velocity in the reach, computed from the data in table 2, the dispersion coefficient, computed from equation 4, is 2.0 m²/s. The ethylene and propane profiles in figure 3 will be discussed later.

Figure 4 is a plot of the observed and computed dye concentrations versus time at points A, B, and C, downstream from Route 820. The computed concentration at point A actually represents the input boundary condition for the model. Again, the model simulations at points B and C reproduce the observed results very well.

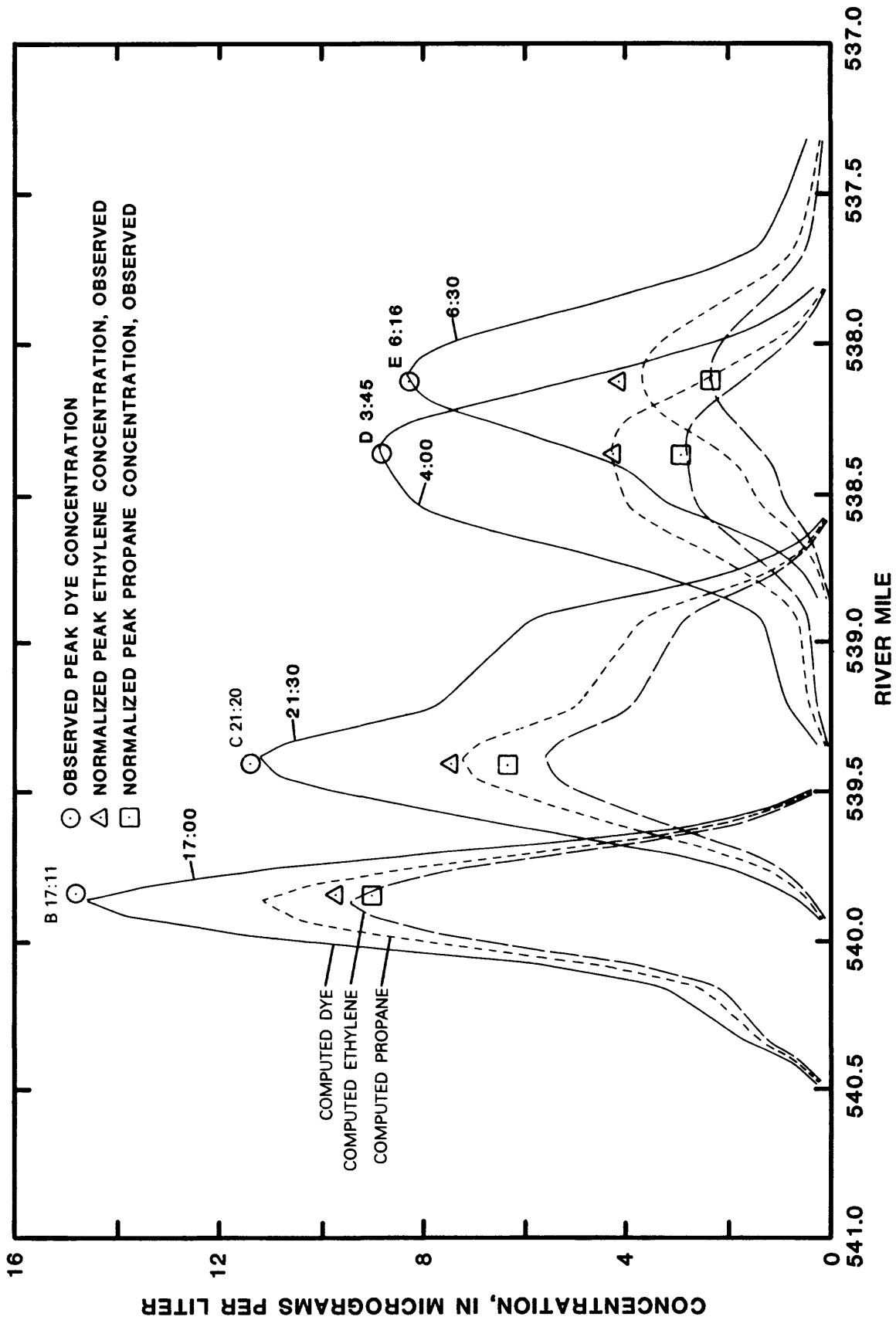


Figure 3. Comparison of observed peak dye and gas concentrations and computed concentrations, West Fork Trinity River downstream from Route 820.

Table 2. Summary of data obtained on the West Fork Trinity River, November 10–13, 1980

Section	Date (1980)	Time	River mile	Peak concentration, in micrograms per liter		
				Dye	Ethylene	Propane
Route 820 injection						
Start Injection	Nov. 10	0953	-----	----	-----	----
Stop Injection	Nov. 10	1100	541.07	----	-----	----
A	Nov. 10	1130	540.80	39.0	132.0	55.4
B	Nov. 10	1711	539.85	14.8	30.4	13.8
C	Nov. 10	2120	539.41	11.4	21.4	10.6
D	Nov. 11	0345	538.37	8.84	9.82	6.09
E	Nov. 11	0616	538.13	8.26	7.84	5.86
Fossil Creek injection						
Start Injection	Nov. 11	1002	-----	----	-----	----
Stop Injection	Nov. 11	1040	543.39	----	-----	----
A	Nov. 11	1205	543.25	21.5	83.5	63.5
B	Nov. 11	1527	542.77	8.23	28.8	23.4
C	Nov. 11	1852	542.51	5.01	13.8	11.6
D	Nov. 11	2145	542.16	3.90	12.5	11.0
E	Nov. 12	0025	542.03	3.58	9.91	9.81
F	Nov. 12	0300	541.94	3.18	8.15	8.11
G	Nov. 12	0620	541.70	3.14	5.80	5.72
Beach Street injection						
Start Injection	Nov. 12	0922	-----	----	-----	----
Stop Injection	Nov. 12	1022	549.60	----	-----	----
A	Nov. 12	1145	549.32	47.0	112.	43.9
B	Nov. 12	1600	548.89	12.8	33.3	13.9
C	Nov. 12	1800	548.73	10.9	22.4	10.4
D	Nov. 13	0040	547.69	8.08	7.12	4.91
E	Nov. 13	0315	547.43	7.75	5.83	4.57
F	Nov. 13	0615	547.15	7.10	-----	-----
G	Nov. 13	1035	546.73	6.72	4.13	4.01
H	Nov. 13	1345	546.30	6.45	3.46	3.72
I	Nov. 13	1645	545.97	6.15	2.86	3.18

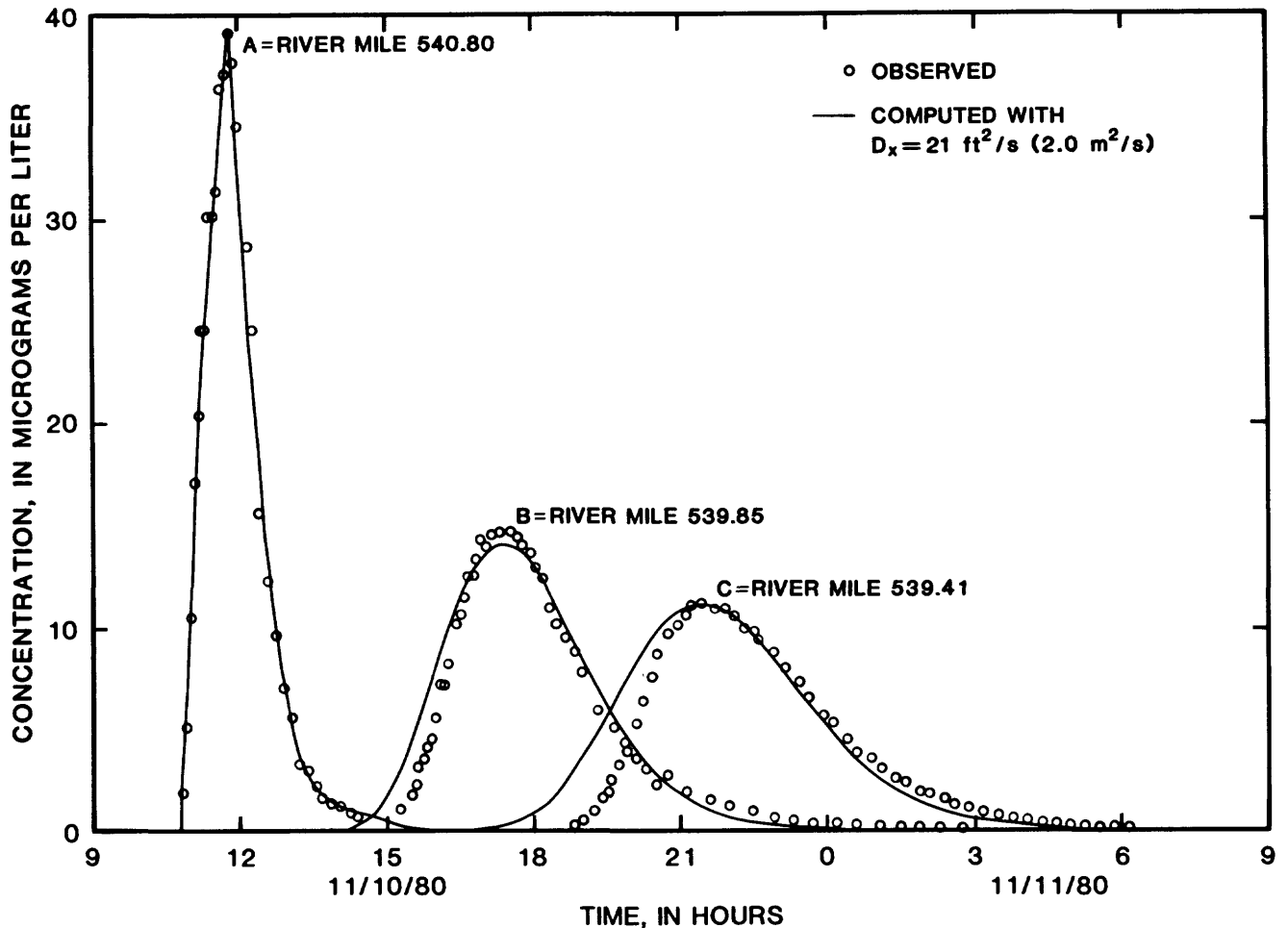


Figure 4. Time variation of observed and computed dye concentrations in the West Fork Trinity River downstream from Route 820.

A comparison of the computed profiles with observed peak concentrations for the Fossil Creek injection is presented in figure 5. The optimum dispersion coefficient was $0.78 \text{ m}^2/\text{s}$. At Fossil Creek and Beach Street, point B was used as the upstream boundary condition because field observations as well as model results indicated that the dye was not fully mixed in the cross section at A. The riffle downstream of point G stretches out the concentration profile. The high-velocity water in this riffle provides a reach nearly a half mile (0.8 km) long which is traversed so rapidly that little longitudinal mixing occurs. The data indicate almost no dispersion between points F and G. These data do not seem to be physically realistic. Although the simulated results do not match the observed data as well as those at Route 820, the results were considered acceptable.

The variation of observed and computed concentrations with time at points B and C for the Fossil Creek in-

jection is shown in figure 6. The results are excellent except that the model under-predicts the tail on the concentration curve at point C. Because of equipment failure, the complete dye curve at point B was not defined. The assumed extensions of the curve at point B may have been a major contributor to the poor fit at point C. Because the dispersion coefficient was determined from only the peak concentration, the accuracy of the extension is of little importance.

Finally, a comparison of the computed profiles with the observed peak concentrations for the Beach Street injection is presented in figure 7. The optimum dispersion coefficient for the Beach Street injection was $1.7 \text{ m}^2/\text{s}$. The riffles near river mile 548.5 and 546.5 distort the concentration profiles. The model provided an excellent estimate of all the peak concentrations for this injection, which was followed for the longest period of time (31 hours) and contained the largest number of observations.

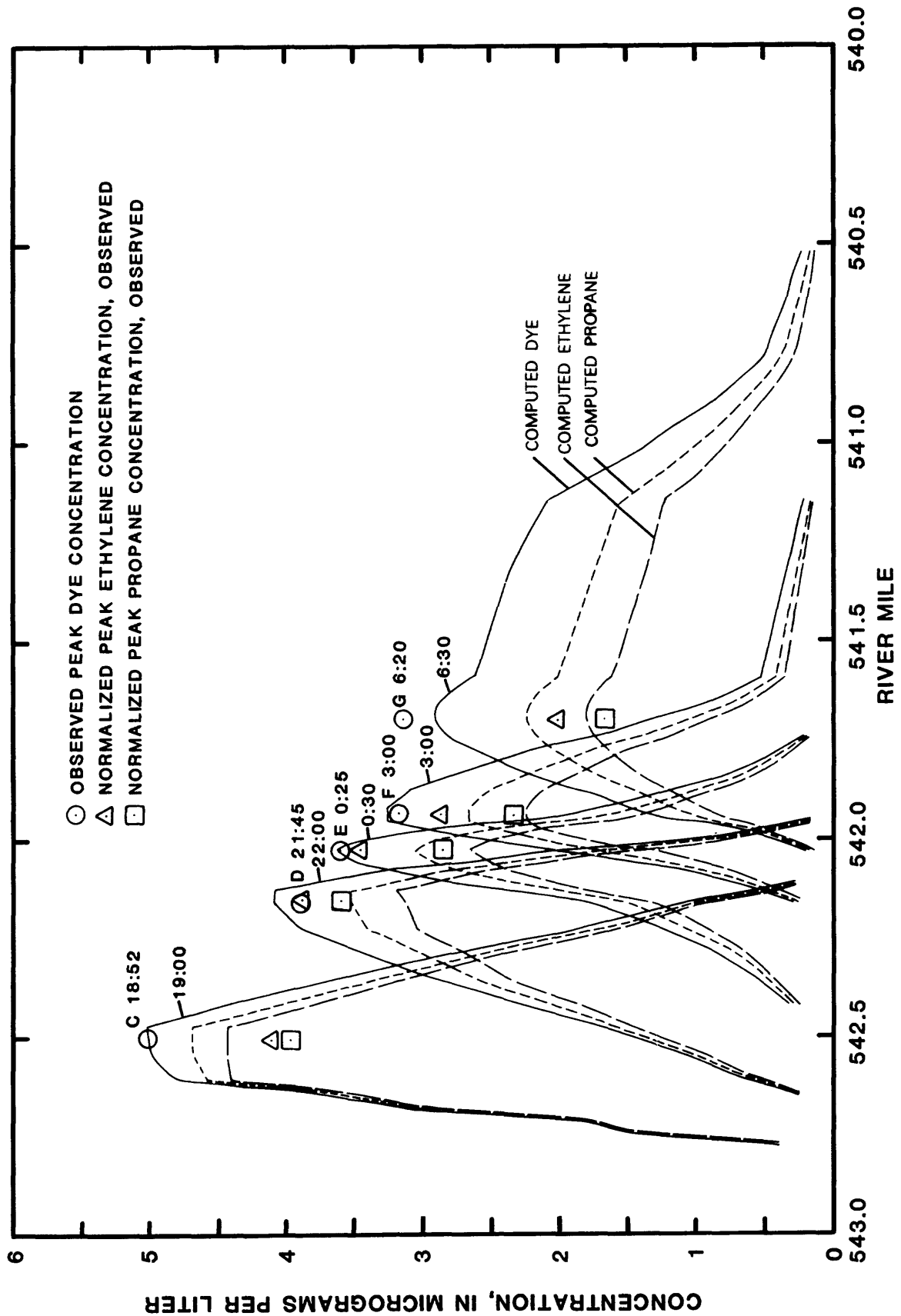


Figure 5. Comparison of observed peak dye and gas concentrations and computed concentrations, West Fork Trinity River downstream from Fossil Creek.

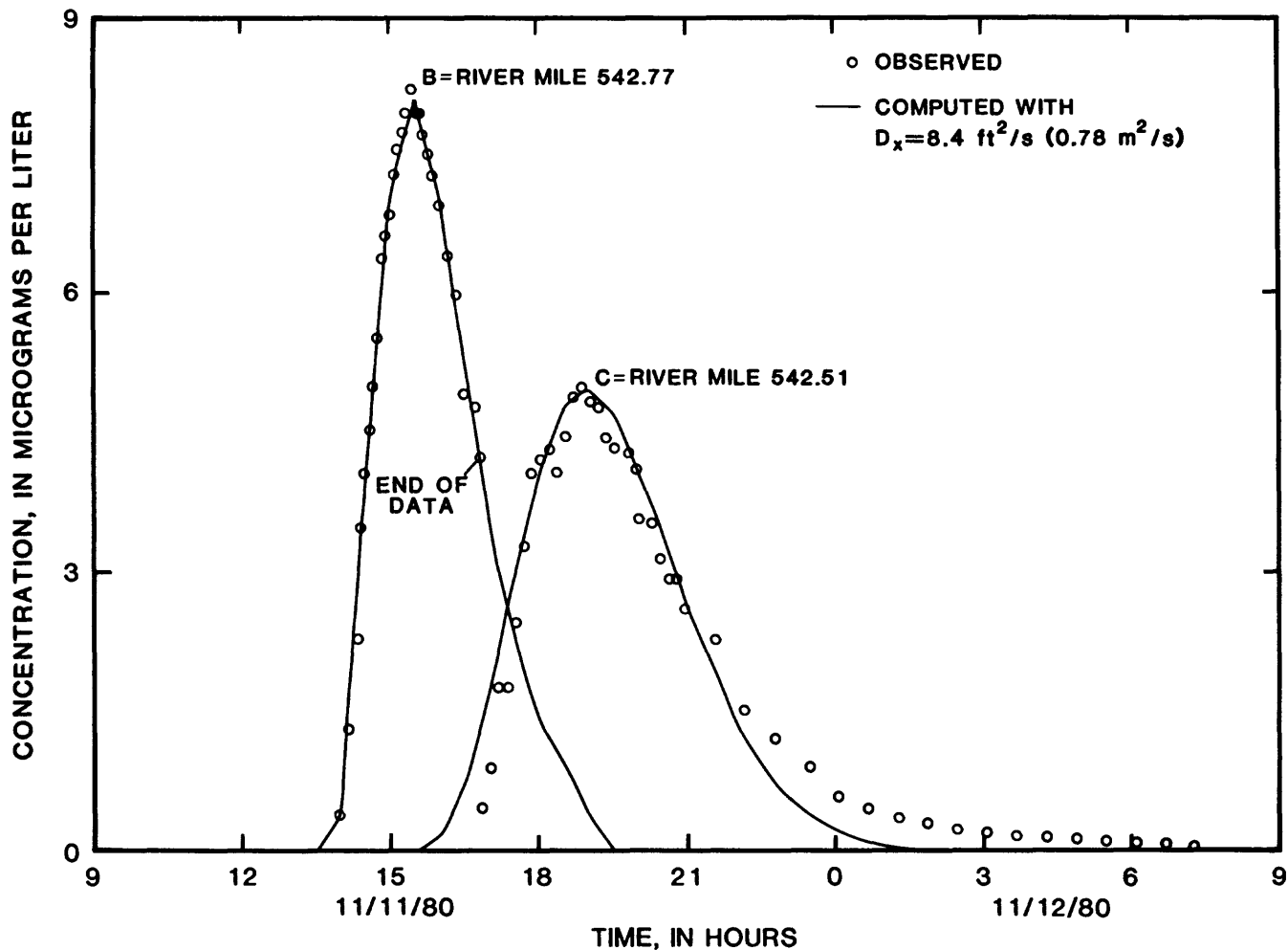


Figure 6. Time variation of observed and computed dye concentrations in the West Fork Trinity River downstream from Fossil Creek.

This injection showed the smallest reduction in peak concentration, even though it was tracked for the longest time. The peak dye concentration of the last point was 48 percent of the initial upstream value, while the final peak values at Fossil Creek and Route 820 were 38 percent and 21 percent, respectively, of the initial values.

The variations of observed and computed concentration with time at points B and C for the Beach Street injection are shown in figure 8. Overall, the results are very good.

The variation of the RMS error with the assumed dispersion coefficient provides an indication of the precision that can be expected in determining the dispersion coefficient using the routing procedure. This variation is shown in figure 9. The RMS error is quite sensitive to the assumed dispersion factor, so the optimum value is well defined.

The river reach traversed by each injection was quite different in character (fig. 2). The Route 820 injection experienced the largest velocity because it traversed several riffles and only small pools. The Fossil Creek injection remained in a single deep pool throughout and had the smallest mean velocity. The Beach Street injection traversed first some riffles then a large pooled section. The dispersion coefficients appear to be reasonably well correlated with velocity, as shown in figure 10, which is a plot of the dispersion coefficients as a function of velocity.

The dispersion coefficients were also computed using the method of moments (Fischer, 1966; Sayre and Chang, 1968) for comparison with values obtained by the routing procedure. Of course, the method of moments can be applied only from point A to point C because it requires a complete concentration versus time curve. Ac-

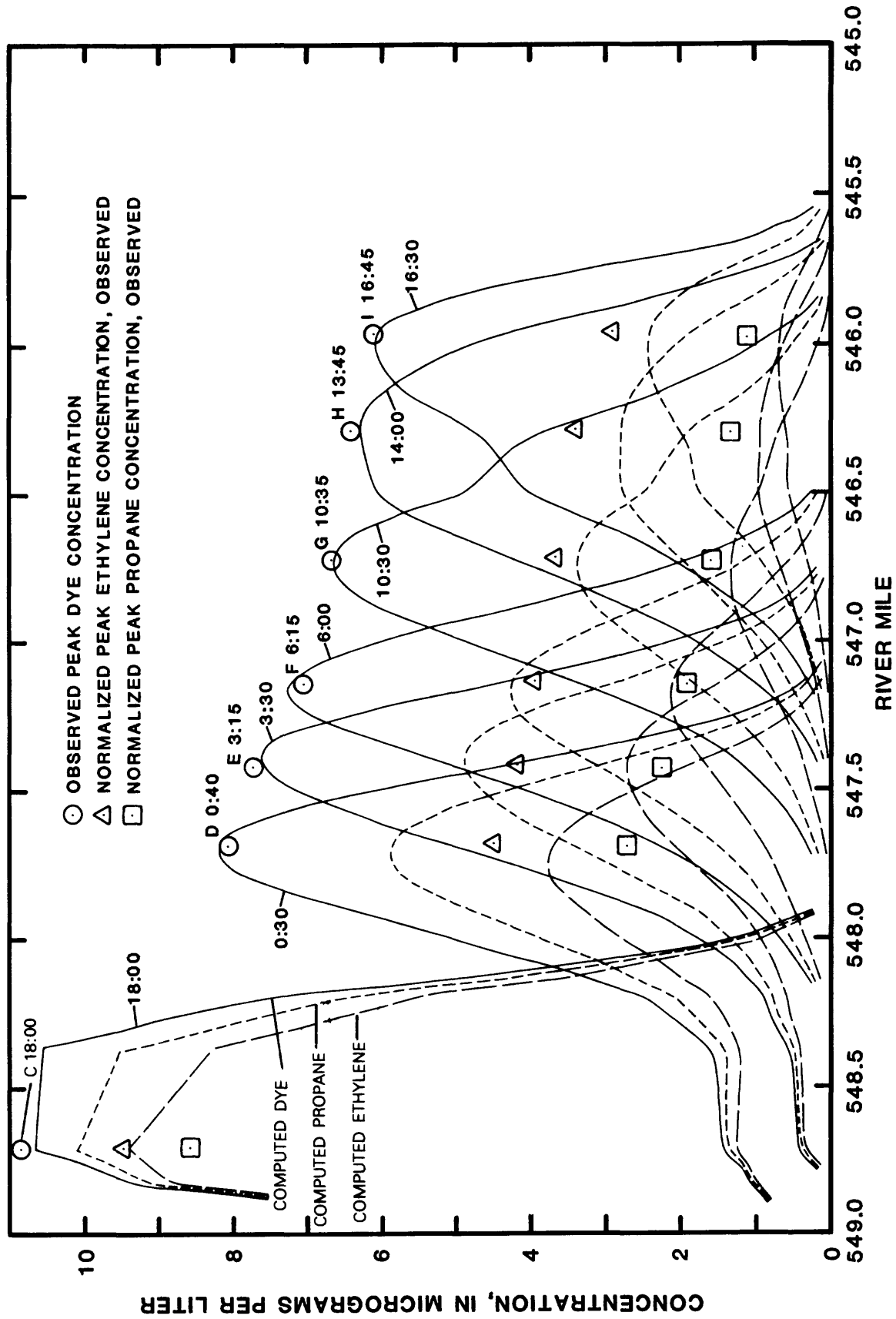


Figure 7. Comparison of observed peak dye and gas concentrations and computed concentrations, West Fork Trinity River downstream from Beach Street.

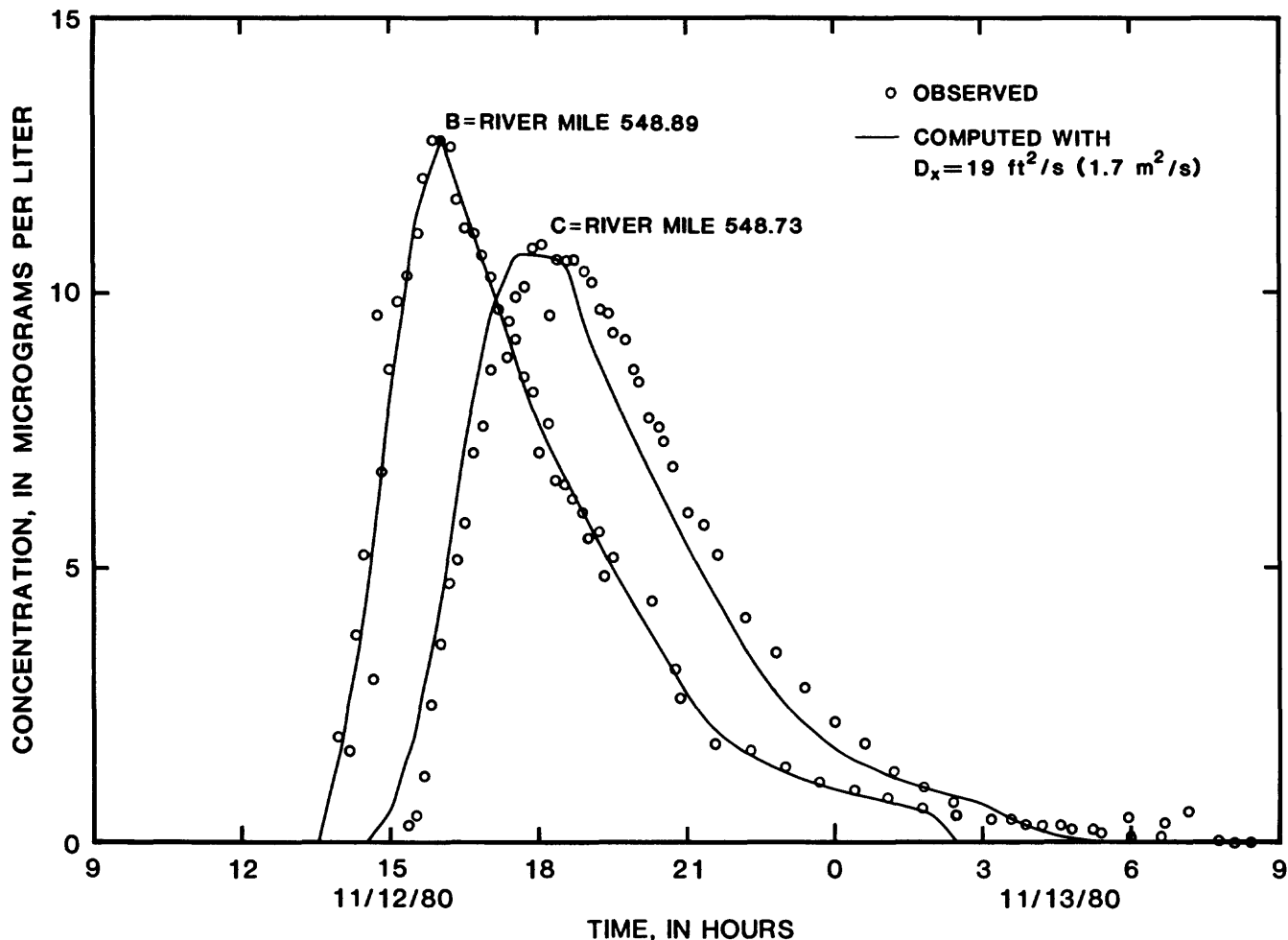


Figure 8. Time variation of observed and computed dye concentrations in the West Fork Trinity River downstream from Beach Street.

According to Fischer (1967), neither the routing procedure nor the method of moments procedure should be applied for short dispersion times. According to the criterion of Fischer, the dispersion time to all points (even point A) was long for all three injections. Because the local depths and shear velocities vary so much, Fischer's criterion is very difficult to apply for a pool and riffle stream such as the Trinity. As Fischer's criterion is satisfied when complete mixing in the cross section occurs, perhaps the qualitative field judgment that cross-sectional mixing was complete, except at point A for the Fossil Creek and Beach Street injections, is a better criterion for applying the method-of-moments procedure.

Applying the method-of-moments procedure between points A and C at Route 820 yielded a dispersion coefficient of $2.1 \text{ m}^2/\text{s}$. The tails on the concentration distributions of observed data (fig. 4) were not excessive, so the results were not very sensitive to where the curves

were truncated. The variance of the concentration distributions also appeared to increase almost linearly with time, indicating that the dye was fully mixed laterally at all three sections. The results, therefore, are believed to be fairly accurate, and the dispersion coefficient agrees very well with the value of $2.0 \text{ m}^2/\text{s}$ obtained by the routing procedure for the reach from points A to E.

At Fossil Creek the method of moments was very difficult to apply. Lateral mixing was not complete at point A, and equipment failure precluded obtaining a complete dye curve at point B. Applying the method of moments between points A and C yielded a dispersion coefficient of $1.9 \text{ m}^2/\text{s}$, which is more than twice as large as the value obtained by the routing procedure. The concentration distribution at point C contained a very long tail in which the concentration remained above 3 percent of the peak concentration. The long tail at point C and the lack of complete mixing at point A would each cause an

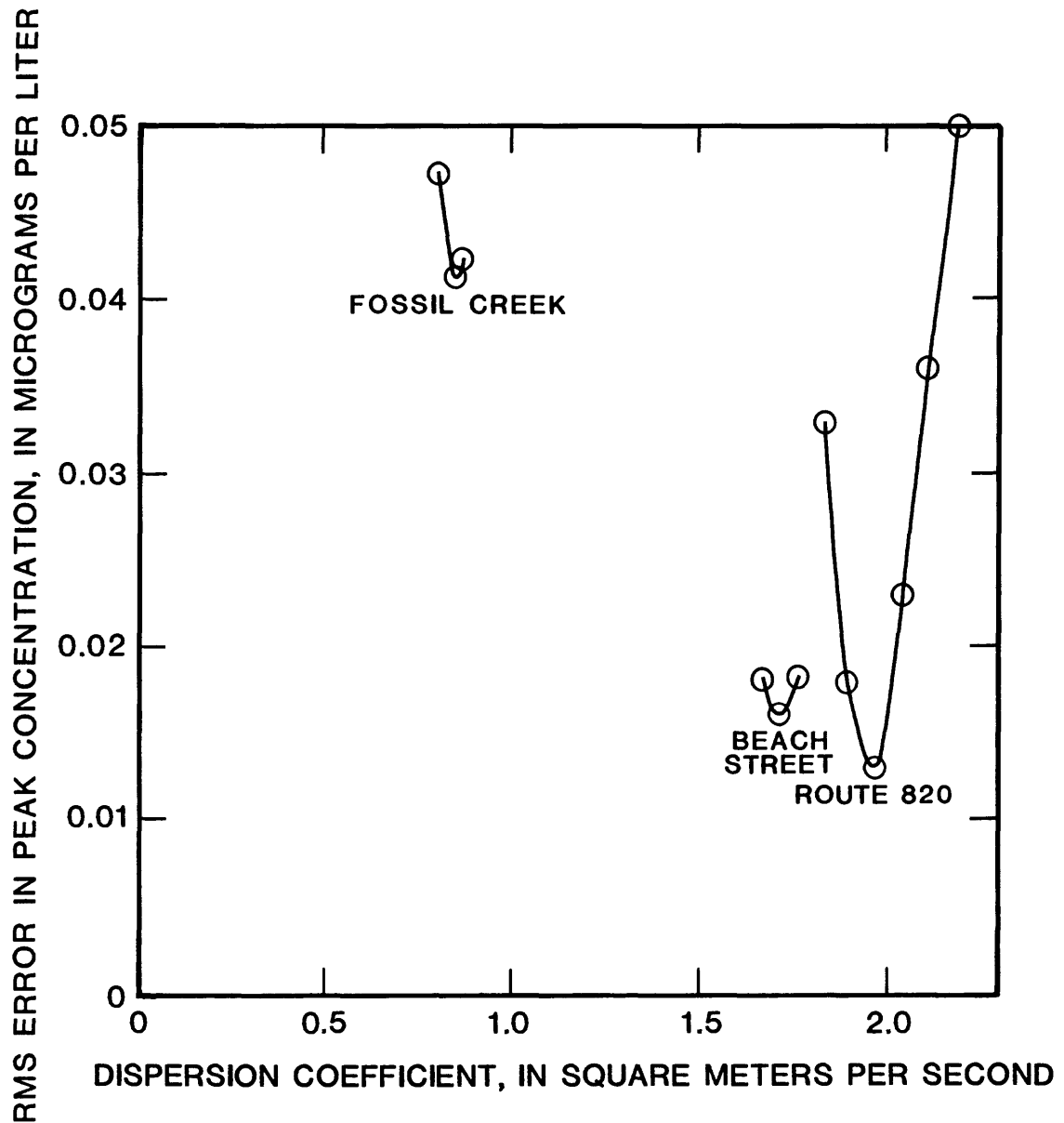


Figure 9. Variation of root-mean-square error in predicted peak dye concentrations as a function of the dispersion coefficient.

increase in the computed dispersion coefficient above the true value. As indicated by Yotsukura and others (1970), if even a small amount of tracer is temporarily trapped in slow-moving flow and subsequently is released to the main flow, it shows up as a tail on the concentration distribution and greatly inflates the value of the dispersion coefficient determined by the method of moments. It is believed that the dispersion coefficient computed for the Fossil Creek injection by the method of moments is unreasonably large.

At Beach Street the method of moments was again difficult to apply because the dye was not laterally mixed at point A. Furthermore, because of a large tail on the curve at point B, the measured variance decreased from points B to C, giving the physically unrealistic result of a negative dispersion coefficient. Applying the method of moments between points A and C yielded a dispersion coefficient of about 2.1 m²/s, which is in fair agreement with the value of 1.7 m²/s obtained by the routing procedure. Because lateral mixing was not complete at point A,

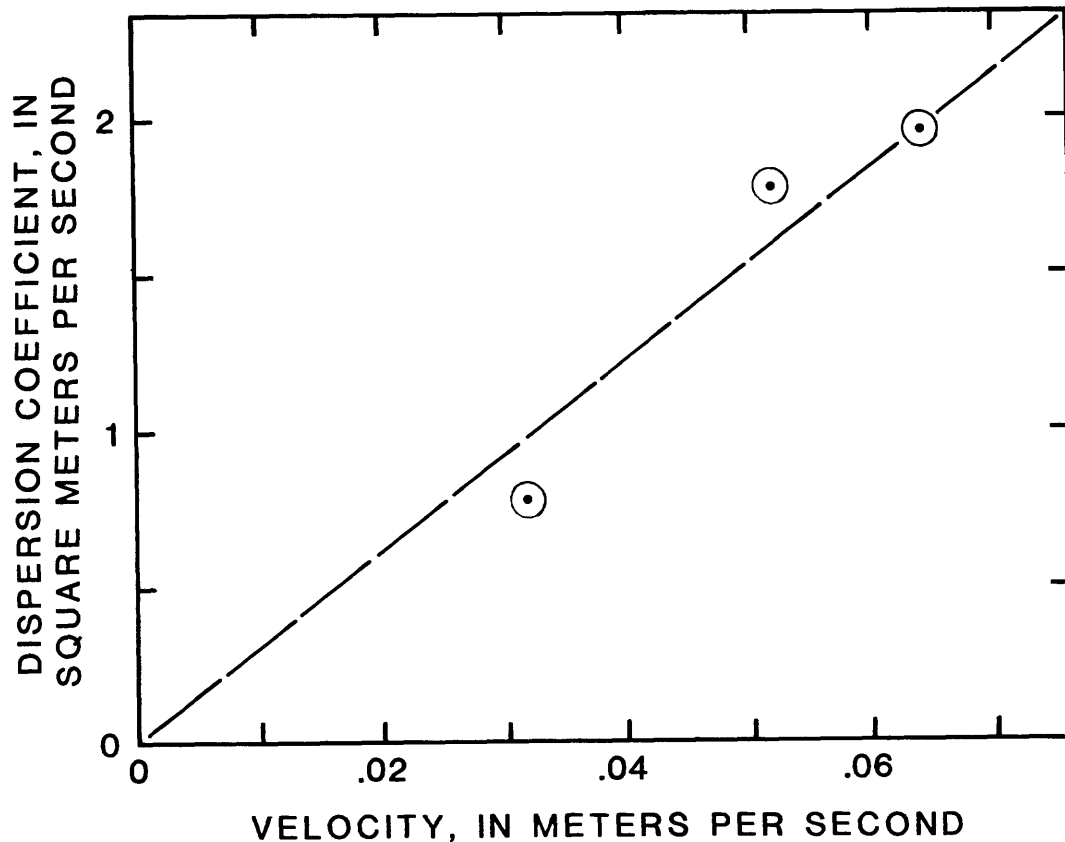


Figure 10. Variation of the dispersion coefficient with mean stream velocity in the West Fork Trinity River.

however, it is believed that the value obtained by the routing procedure is more representative.

In summary, it appears that the dispersion coefficients obtained by the routing procedure and the method of moments are of comparable value when the method of moments gives reliable results. Furthermore, the Lagrangian model appears to have simulated the dye concentration in the river very well for all three injections.

Desorption

The concentration of gas dissolved in water depends on the rate of dispersion and the rate of desorption at the surface. Once the model is accurately simulating the dispersion process, it is possible to use it and the routing procedure to determine the desorption coefficients. Equation 5 was used to simulate the concentration of ethylene and propane.

The concentration of gas at the upstream point was assumed to be proportional to the dye concentration at that point, with the ratio of the observed peak concentrations from table 2 as the proportionality constant. The liquid

film coefficient (equation 7) was varied until the RMS error between the computed and observed peak concentrations was minimized. The resulting coefficients are presented in table 3 along with the resulting RMS error. The gas profiles predicted by the mass—transfer model and the observed peaks are shown in figures 3, 5, and 7. In these figures, the gas concentrations have been normalized such that the masses of gas and dye passing the upstream boundary are equal. Because without desorption the gas curves would be identical to the dye curves, normalization allows one to visualize the amount of gas that is lost to the atmosphere.

Although the scatter in the gas concentrations is larger than that in the dye concentrations (two sources of error are present here), the model does a good job of predicting the observed gas concentrations. The liquid film coefficients in table 3 represent a value which best describes the peak gas concentrations in the RMS sense.

Optimum desorption coefficients obtained using the bulk-transfer model are also presented in table 3. The predicted concentration profiles using the bulk-transfer model were very similar in appearance to those in figures 3, 5, and 7.

Table 3. Results of model calibration on West Fork Trinity River

Injection	Constituent	Mean velocity, in feet per second	Dispersion		Mass transfer		Bulk transfer	
			Coef- ficient, in square feet per second	RMS error, in micro-gram per liter	Liquid- film coef- ficient, in feet per day	RMS error, in micro-gram per liter	Desorp- tion coef- ficient, per day	RMS error, in, micro-gram per liter
Route 820	Dye	0.21	21	0.013	---	-----	---	-----
	Ethylene	----	---	-----	4.0	0.066	1.6	0.075
	Propane	----	---	-----	2.5	.085	1.0	.106
Fossil Creek	Dye	0.11	8.4	.041	---	----	---	-----
	Ethylene	----	---	-----	3.6	.090	.82	.080
	Propane	----	---	-----	2.0	.109	.45	.104
Beach Street	Dye	.17	19	.016	---	----	---	-----
	Ethylene	----	---	-----	6.9	.245	2.2	.289
	Propane	----	---	-----	3.0	.171	.94	.189

When using the peak method (Rathbun and others, 1975) for computing the desorption coefficients, one must assume the bulk-transfer model because the depth cannot be accounted for independently. Determining the desorption coefficients for ethylene and propane on a reach-by-reach basis yielded very erratic results because of the small changes in the observed concentrations from point to point. To determine overall desorption coefficients by the peak method comparable to those given in table 3, the logarithms of the ratio of gas to dye concentrations were plotted as a function of travel time and a least squares line was fit to the data. The slope of the fitted line was equal to the desorption coefficient. The resulting desorption coefficients for ethylene were 1.6, 0.89, and 1.6 per day, for the injections at Route 820, Fossil Creek, and Beach Street, respectively. The desorption coefficients for propane were 0.94, 0.50, and 0.62 per day for the injections

at Route 820, Fossil Creek, and Beach Street, respectively. These values differ somewhat from the values given in table 3. There are two reasons for the difference. The main reason, especially for the difference for the Beach Street injection, was that the fitted curve with the peak method had two degrees of freedom, the intercept and the desorption coefficient, whereas the routing procedure had only one degree of freedom, the desorption coefficient. The initial condition, the concentration at the first point, was assumed to be exact. When the peak method was constrained to fit the first point, the results were almost the same by either method. The slight differences that did occur resulted because the peak method yields a coefficient that minimizes the error in the logarithm of the ratios of the peak gas to dye concentrations, while the routing procedure minimized the error in the computed concentrations.

Evaluation of the Model

The curves shown in figures 3, 4, 5, 6, 7, and 8 indicate that the model provides an excellent description of the dispersive process in the West Fork Trinity River. Considering the extremely non-uniform nature of the river flow area, this is perhaps surprising. The dispersion coefficient (fig. 10) seems to be related to mean stream velocity. With a steady flow of about $0.76 \text{ m}^3/\text{s}$, the dispersion coefficient in the West Fork Trinity River varies from about $0.7 \text{ m}^2/\text{s}$ in deeply pooled areas below Fossil Creek to about $2.0 \text{ m}^2/\text{s}$ in the riffled sections below Route 820.

Although the dispersion coefficient is larger in the riffled sections of the river, the rate of decrease in the peak dye concentration with distance is larger in the pooled areas than in the riffles. For example, the peak concentration fell at an average rate of 38 percent per kilometer for the pooled region of Fossil Creek when the dispersion coefficient was $0.78 \text{ m}^2/\text{s}$. In the riffled section at Route 820, however, where the dispersion coefficient was $2.0 \text{ m}^2/\text{s}$, the peak dye concentration decreased at an average rate of only 18 percent per kilometer. The dispersive flux is equal to the product of the dispersion coefficient and the concentration gradient (equation 1). Figures 3, 5, and 7 illustrate the effect of the riffles on the longitudinal concentration profiles. The riffles essentially stretch out or elongate the water parcels so that the concentration gradient is much reduced. Because the peaks decay more slowly in the riffles, this reduction in concentration gradient must more than compensate for the increased turbulence and the larger dispersion coefficient. The pools, on the other hand, compress the concentration profile, giving much larger gradients. Judging from the results at Beach Street, which contains both riffles and pools, the model does an excellent job of accounting for this process.

As indicated in figure 9, the routing procedure using a Lagrangian type model is robust because the computed results are very sensitive to the assumed dispersion coefficient. This procedure is independent of the judgment of the analyst and is not sensitive to the tails on the concentration curves, which cause so much difficulty when applying the method-of-moments procedure. In all cases in which the method-of-moments procedure was believed to be accurate, the dispersion coefficient agreed very closely with the value obtained by the routing procedure.

In summary, the determination of a dispersion coefficient using the method-of-moments procedure requires extensive field data, and the results tend to be erratic and quite sensitive to the judgment of where the tails of the concentration curves are truncated. The routing method using a Lagrangian transport model is robust and is not sensitive to the judgment of the analyst. By fitting the routing procedure to peak concentrations, only a relatively

small amount of easily obtained data is required, with little sacrifice in the accuracy of the results. It is suggested that a tremendous amount of labor could be saved in time-of-travel or dispersion studies for a small sacrifice in accuracy by tracing the peak concentrations at more or less fixed time intervals rather than measuring complete dye curves at fixed points.

The routing and the peak methods provided nearly the same estimates of the bulk-transfer desorption coefficients. Although the routing procedure is more involved, it can be used for unsteady flows and provides much greater flexibility in analysis by accounting for tributary inflow automatically as well as by allowing the desorption coefficient to be a function of independent variables such as wind speed. The only data actually required by either procedure are the peak dye and gas concentrations along the river at various times. Of course, the locations of the peak concentrations must also be known for the routing procedure.

The bulk-transfer coefficient for propane averaged about 50 percent of the ethylene value. In stirred tank experiments, the desorption coefficient of propane averaged 81 percent of the ethylene value (Rathbun and others, 1978). The reason for the difference in the ratios between the stirred tank and the river is not known.

The reach-to-reach variation of the liquid film coefficient in table 3 is similar to the reach-to-reach variation of the desorption coefficient. The value below Fossil Creek is always the smallest of any of the injections and, except for one case, the value at Beach Street is the largest. If the physical—chemical factors that control gas desorption were completely described by equations 6 and 7, one would expect the liquid film coefficient to be a constant for either gas. The reach-to-reach variation in the liquid film coefficient, although large, is smaller than the reach-to-reach variation in the desorption coefficient.

Another measure of the adequacy of a particular model is RMS error in the computed peak gas concentration, which is also tabulated in table 3. In terms of the RMS error, the mass-transfer model (liquid film coefficient) provides a better description of the data at Route 820 and Beach Street while the bulk-transfer model provides a better description of the Fossil Creek data. The mass-transfer model provides a depth correction (equation 7), while the bulk-transfer model does not. At Fossil Creek, the tracers remained in a single large pool during their entire transit wherein the percentage change in depth was small compared with the changes in the other reaches.

The mass-transfer approach is believed to be a better model of the desorption process because the liquid film coefficient is more consistent reach to reach and because, in general, the RMS errors produced by that model are smaller than those produced by the bulk-transfer model.

Tsivoglou and Wallace (1972) state that reaeration (or desorption) is directly proportional to the head loss and

inversely proportional to the time of travel through a reach. Since the head loss generally increases with increasing velocity and decreasing depth, the model of Tsivoglou and Wallace, like the mass-transfer model, indicates that the desorption coefficient should be larger in shallow areas than in deep areas.

Comparison of the mean velocities from table 3 and the plotted depths on figure 2 indicates that the Fossil Creek reach could be classified as containing pools, the Route 820 reach as containing many riffles, and the Beach Street reach as containing riffles above point D and pools below point D. The liquid film coefficient was smallest for the pooled reach at Fossil Creek and increased in the riffled reaches. It appears that the desorption coefficient varies more with depth or velocity than indicated by the mass-transfer model.

The results for the Beach Street injection also suggest that the desorption coefficient varies more with depth than indicated by the mass-transfer model. The values given in table 3 are much larger than for the other two reaches, even though the hydraulic characteristics of the Beach Street reach seemed to fall between the values for the other two reaches. Figure 7 indicates that a much higher gas loss is needed between points B and D than the model predicts and that a much lower loss rate is needed between points D to I. Starting the model at point D yielded coefficient values between those obtained at Route 820 and Fossil Creek, which appears consistent with the depths of this reach shown in figure 2. Either the mass-transfer approach does not adequately account for the shallow flow in the riffles near river mile 548 or the model overestimates water depth. The effective water depths in the riffles were, unfortunately, based on very crude observations. The rate of dispersion was not directly related to water depth, and the dye concentrations were predicted well through the riffle.

In summary, it appears that the mass-transfer model provides a better description of the desorption process than the bulk-transfer model but that even the mass-transfer model does not adequately allow for changes in hydraulic conditions such as depth.

SUMMARY AND CONCLUSIONS

Dispersion and desorption coefficients were determined from data collected on the West Fork Trinity River near Fort Worth, Tex. Data were analyzed using a routing procedure as well as standard techniques. The following conclusions are drawn from the study.

1. At a steady flow of about $0.76 \text{ m}^3/\text{s}$, the dispersion coefficient varied from a low of about $0.7 \text{ m}^2/\text{s}$ in the deep pools below Fossil Creek to about $2.0 \text{ m}^2/\text{s}$ in the riffles and small pools below Route 820.

2. Using a Lagrangian transport model to minimize numerical dispersion, the routing procedure provides more consistent estimates of the dispersion coefficient than the method of moments.
3. Applying the routing procedure to only the peak dye concentrations yielded dispersion coefficients within 10 percent of the values obtained when it was applied to the entire concentration-time curves. It is much easier to obtain peak dye concentrations than to obtain the complete dye curves.
4. The Lagrangian transport model provided an excellent description of the dispersion process, even in the extremely pooled and riffled reach of the West Fork Trinity River below Fort Worth.
5. The desorption coefficient can be determined using either the routing procedure or the standard peak method with essentially the same accuracy.
6. At a steady flow of about $0.76 \text{ m}^3/\text{s}$, the liquid-film coefficient for ethylene and propane varied from a low in the pooled reaches to a higher value in the riffled reaches. Specific values for individual reaches are presented in table 3.
7. At the same flow, the bulk-transfer coefficient for ethylene and propane also varied from a low value in the pooled reaches to a higher value in riffled reaches. Specific values for individual reaches are presented in table 3.
8. The liquid film coefficient varies less from reach to reach than the bulk-transfer coefficient, indicating that the mass-transfer model is a better description of the desorption process in natural streams. However, even the mass-transfer model does not adequately compensate for changes in hydraulic conditions such as depth changes.

REFERENCES

- Carslaw, H. S., and Jaeger, J. C., 1959, *Conduction of heat in solids*, (2d ed.): New York, Oxford University Press, 101 p.
- Fischer, H. B., 1966, A note on the one-dimensional dispersion model: *Air and Water Pollution, an International Journal*, v. 10, p. 443-452.
- 1967, The mechanics of dispersion in natural streams: *American Society of Civil Engineers, Journal of Hydraulics Division*, v. 93, no. HY 6, p. 187-216.
- 1968, Dispersion predictions in natural streams: *American Society of Civil Engineers, Journal of Sanitary Engineering Division*, v. 94, no. SA 5, p. 927-943.
- Jobson, H. E., 1980, Comment on 'A new collocation method for the solution of the convection-dominated transport equation' by George E. Pinder and Allen Shapiro: *Water Resources Research*, v. 16, no. 6, p. 1135-1136.
- 1981, Temperature and solute-transport simulation in streamflow using a Lagrangian reference frame: *U.S. Geological Survey Water-Resources Investigations* 812, 165 p.

- Rathbun, R. E., Shultz, D. J., and Stephens, D. W., 1975, Preliminary experiments with a modified tracer technique for measuring stream reaeration coefficients: U.S. Geological Survey Open-file Report 75-256, 36 p.
- Rathbun, R. E., Stephens, D. W., Shultz, D. J., and Tai, D. Y., 1978, Laboratory studies of gas tracers for reaeration: American Society of Civil Engineers Proc., Journal of Environmental Engineering Division, v. 104, no. EE2, p. 215-229.
- Sayre, W. W., and Chang, F. M., 1968, A laboratory investigation of open-channel dispersion processes for dissolved, suspended, and floating dispersants: U.S. Geological Survey Professional Paper 433-E, 71 p.
- Tsivolgou, E. C., and Wallace, J. R., 1972, Characterization of stream reaeration capacity: U.S. Environmental Protection Agency report no. EPA-R3-72-012, Washington, D.C., October, 317 p.
- Yotsukura, Nobuhiro, Fischer, H. B., and Sayre, W. W., 1970, Measurement of mixing characteristics of the Missouri River between Sioux City, Iowa, and Plattsmouth, Nebraska: U.S. Geological Survey Water-Supply Paper 1899-G, 29 p.

Metric Conversion Factors

Data listed in this reported are defined in metric units. A list of these units and the factors for their conversion to inch-pound units is provided below.

Abbreviations of units are defined in the conversion table below or where they first appear in the text. Symbols are defined where they first appear in the text.

Multiply metric units	By	To obtain inch-pound units
cubic meter per second (m ³ /s)	35.31	cubic foot per second (ft ³ /s)
meter (m)	3.28	foot (ft)
square meter (m ²)	10.76	square foot (ft ²)
millimeter (mm)	0.03937	inch (in.)
square kilometer (km ²)	0.3861	square mile (mi ²)
kilometer	0.6214	mile